# The Physical Properties of Carbon Nanoparticles Dispersed into NBR/LLDPE Nanocomposites for Corrosion Protection Applications

**Waleed E. Mahmoud**

*Faculty of Science, Department of Physics, King Abdul-Aziz University, Jeddah, Saudi Arabia*

Received 25 January 2011; accepted 10 April 2011
DOI 10.1002/app.34665
Published online 31 August 2011 in Wiley Online Library (wileyonlinelibrary.com).

**ABSTRACT:** In this study, novel acrylonitrile butadiene rubber (NBR) nanocomposites with improved electrical conductivity and mechanical properties were synthesized. Carbon nanoparticles (CNP)/NBR composites and CNP-polyethylene/NBR nanocomposites were prepared by mixing via two-roll mill. The first type of the nanocomposite was produced to determine the percolation threshold concentration ($V_c$). The second type with constant CNP concentration, slightly over $V_c$ (0.2 vol %), was synthesized to investigate the influence of polyethylene content on the mechanical, electrical and swelling behavior of nanocomposites. Only the nanocomposites with 3 vol % polyethylene loading showed electrical conductivity. However, the composites with higher polyethylene loadings showed insulating behavior due to hindrance of CNP network by polyethylene layers. Swelling measurements revealed that the change in entropy of the swelling increased with the increase in disorder level but decreased with the increase in intercalation level of CNP in the disordered intercalated nanocomposite. The increase in solvent uptake was comparable with the free volume in NBR matrix upon inclusion of nanoparticles, whereas the inhibition in solvent uptake for higher polyethylene loading was described by bridging flocculation. © 2011 Wiley Periodicals, Inc. J Appl Polym Sci 123: 2667–2675, 2012

**Key words:** nanocomposites; swelling; modification

## INTRODUCTION

Inexpensive inorganic substances are traditional ingredients in polymer industry. They are widely used as fillers to improve mechanical[1] and thermal properties[2] of polymers and polymer composites, to decrease shrinkage and internal stresses during fabrication of polymer articles, to increase thermal conductivity,[3] thermal stability,[4] flame resistance,[5,6] and, not of least importance, to improve cost effectiveness.[7] The last motivation often became the most important one despite some deterioration of properties with immoderate filling of polymer or polymer composite.

Hybrid polymer-inorganic nanocomposite materials are promising for a variety of applications. Because of their unique electronic,[8] optical,[9] and mechanical properties,[10,11] they have attracted the particular attention of researchers and engineers in recent decades. Major changes in the understanding of inorganic particles and corresponding hybrid polymer-inorganic composite material applications occurred when physicists, chemists, and material scientists realized that reduction in dimensions of the particles results in the appearance of a new crystal motif, or perhaps a new physical phenomenon that does not exist in materials with larger grain sizes.

Corrosion protection using conductive polymers was first suggested by MacDiarmid.[12] Almost all of the conductive polymers used in corrosion protection fall under the following classes: polyanilines, polyheterocycles and poly(phenylene vinylene)s. conductive polymers can be synthesized both chemically and electrochemically. It has been observed that most conductive polymers can be electrochemically produced by anodic oxidation,[13] enabling one to obtain a conducting film directly on a surface. conductive polymers can go from the insulating to the conducting state through several doping techniques such as chemical doping by charge transfer, electrochemical doping, doping by acid-base chemistry (only polyaniline undergoes this form of doping), photodoping and charge injection at a metal-semiconducting polymer interface.[14] The present work represents a novel contribution for preparing rubber composite loaded carbon nanoparticles (CNP) modified with linear low density polyethylene (LLDPE) to be used as a coating material for metals to inhibit the corrosion effect.

## EXPERIMENTAL

### Materials and processing

Acrylonitrile butadiene rubber (NBR) (density 0.98 g/cm$^3$ and acrylonitrile content 26%) and LLDPE

*Permanent address:* Physics department, Faculty of Science, Suez Canal University, Ismailia, Egypt. (w_e_mahmoud@yahoo.com).

**TABLE I**
**Ingredients of the Investigated NBR Rubber Nanocomposites**

| Ingredients (g) | N1 | N2 | N3 | N4 | N5 | N6 |
|---|---|---|---|---|---|---|
| NBR | 100 | 100 | 100 | 100 | 100 | 100 |
| Stearic acid | 2 | 2 | 2 | 2 | 2 | 2 |
| Zinc oxide | 5 | 5 | 5 | 5 | 5 | 5 |
| CNP | 0 | 1 | 2 | 3 | 4 | 5 |
| DOP | 10 | 10 | 10 | 10 | 10 | 10 |
| MBTS | 2 | 2 | 2 | 2 | 2 | 2 |
| PBN | 1 | 1 | 1 | 1 | 1 | 1 |
| Sulfur | 2.5 | 2.5 | 2.5 | 2.5 | 2.5 | 2.5 |

(density 0.92 g/cm$^3$ and average molecular weight 38,000) were used as polymer matrices. CNP (10 nm diameter) were used as reinforcing filler. Other compounding ingredients like zinc oxide and stearic acid (activators), Dibenz thiazyl disulphide (MBTS) semiultra accelerator (vulcanization time 30 min at temperature 150°C), Phenyl-β-naphthyl-amine (PBN) antioxidant (melting point 105°C), Dioctyle phthalate (DOP) plasticizer and sulfur (vulcanizing agent) were used. These materials were compounded according to the recipe listed in Table I. In case of NBR/PE blend, the materials were compounded according to the recipe listed in Table II.

For the compounding, a homemade two-roll mixing mill (length 0.3 m, radius 0.15 m, speed of slow roll 18 rpm and gear ratio 1.4) was used. The mixing occurred for 40 min at a temperature of 25°C. The compounded rubbers were compression molded into cylinders of $1 \times 10^{-4}$ m$^2$ area and 0.01 m in height. The vulcanization were conducted under a heating press (KARL KOLB, Germany) at a pressure of $P =$ 0.40 MPa. The optimum conditions of temperature and time were $T = 150$°C and $t = 30$ min.[15,16] The vulcanized samples were shelf aged for 48 h before test. The mixing time and vulcanization conditions were fixed for all samples.

### Measurements

The stress–strain behavior was measured at room temperature by using a material tester (AMETEK, USA), which connected by a digital force gauge (Hunter Spring ACCU Force II, 0.01$N$ resolutions, USA) to measure stress forces. The force gauge interfaced with computer to record the obtained data. The stress–strain behavior was measured at strain rate 1 mm/s. The samples were in form of strips (length 2 cm, width 2 mm, and thickness 1.2 mm). For electrical measurements, brass electrodes were attached to the parallel faces of the samples during vulcanization and digital electrometer (616 Keithly, USA) was used.

Circular shaped samples (diameter $\sim$ 12 mm) were cut from the block copolymer sheets and the thickness of the samples was measured with an accuracy of $\pm$0.01 mm. Dry weight of the cut samples were taken before immersion into gasoline solvent at room temperature. The samples were periodically removed from test bottles and the adhering solvent blotted off the surface. Then the samples were weighed on an electronic balance (Shimadzu, Libor AEU-210, Japan) and immediately replaced into the test bottles. This procedure was continued until equilibrium swelling was attained in the case of each sample. The time taken for each weighing was kept constant to a minimum of 20–30 s to avoid errors due to the escape of solvent from the samples. The results of these experiments were expressed as the amount of solvent uptake by polymer sample according to the relation, $Q_t$ (mol %) $= (m_t - m_o/m_o) \times 100\%$, where $m_o$ is the mass of polymer sample before swelling test and $m_t$ is the mass of polymer after swelling at time $t$.

## RESULTS AND DISCUSSION

### Electrical properties

The electrical properties of CNP/NBR composites were characterized in terms of electrical conductivity and related percolation theory. The dependence of direct current (dc) conductivity at room temperature on CNP concentration is seen in Figure 1

The behavior of conductivity can be described in terms of percolation phenomena.[17–19] At a critical filler concentration, the characteristic percolation threshold transition occurs. Percolation threshold concentration is defined as the critical CNP volume fraction ($V_c$) where the conducting network is formed and the electrical conductivity is within static dissipative range of $10^{-5}$ to $10^{-4}$ S cm$^{-1}$. The percolation threshold concentration was measured to be about 0.175 vol % CNP loading. Hence for concentrations of 0.175 vol % and above, the composite is called electrically conductive. The $V_c$ value measured was found to be lower compared with the other works reported in the literature.[20] Low values

**TABLE II**
**Ingredients of the Investigated NBR/LLDPE Nanocomposites**

| Ingredients | 1 vol % | 3 vol % | 5 vol % | 7 vol % | 9 vol % |
|---|---|---|---|---|---|
| NBR | 100 | 100 | 100 | 100 | 100 |
| LLDPE (vol %) | 1 | 3 | 5 | 7 | 9 |
| Stearic acid | 2 | 2 | 2 | 2 | 2 |
| Zinc oxide | 5 | 5 | 5 | 5 | 5 |
| CNP (vol %) | 0.2 | 0.2 | 0.2 | 0.2 | 0.2 |
| DOP | 10 | 10 | 10 | 10 | 10 |
| MBTS | 2 | 2 | 2 | 2 | 2 |
| PBN | 1 | 1 | 1 | 1 | 1 |
| Sulfur | 2.5 | 2.5 | 2.5 | 2.5 | 2.5 |

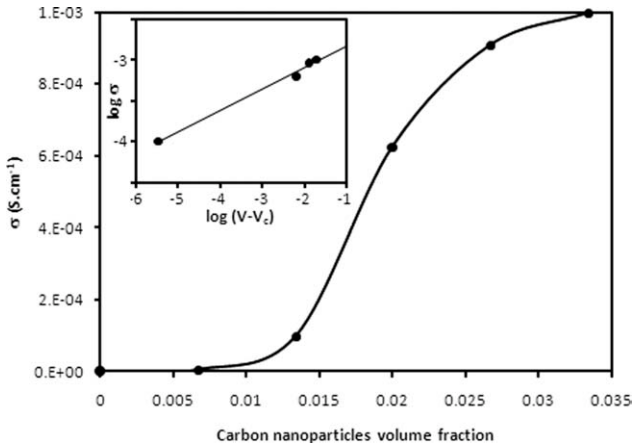


**Figure 1** Conductivity against carbon nanoparticles volume fraction.

of $V_c$ are related to highly structured CNP network formation in the corresponding polymers.

The dc conductivity of such insulator-conductor composites near percolation threshold follows universal scaling laws given below[21];

$$\sigma_{dc}\alpha(V - V_c)^t, \quad \text{for } V > V_c, \tag{1}$$

where $\sigma_{dc}$ is the direct current electrical conductivity, $V$ is the CNP concentration (vol %), $V_c$ is the percolation threshold concentration (vol %), and $t$ is the critical exponent for three-dimensional structures. Values of $t$ should be in the range of l.7–2.0.[22,23] "$t$" is determined from the slope of the best fitting of $\sigma_{dc}$ versus $(V - V_c)$ as shown inset of Figure 1. It was found that $t = 1.98$. The critical exponent "$t$" was in the range stated, between 1.7 and 2. This means, CNP/NBR nanocomposites follow power-law behavior. Based on the results in Figure 1, CNP concentration of 0.2 vol % which was slightly above the $V_c$ was chosen and kept constant for the production of CNP-modified polyethylene nanocomposites.

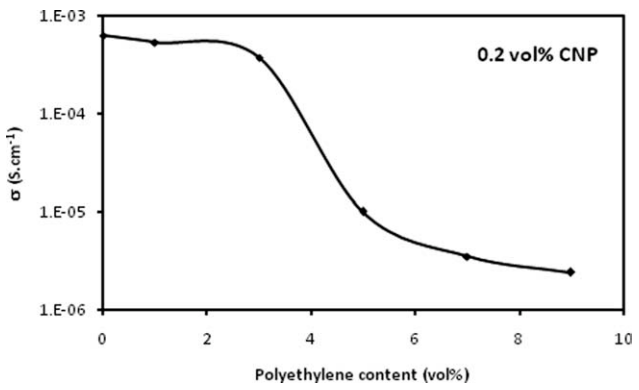


**Figure 2** Conductivity against polyethylene content at fixed 0.2 vol % carbon nanoparticles.

The effect of polyethylene content on conductivity of nanocomposites loaded 0.2 vol % of CNP is shown in Figure 2. It was found that the conductivity of the nanocomposites is marginal up to 3 vol % and then decreases with more addition polyethylene. One can conclude that, a small amount of polyethylene up to 3 vol% did not affect on the conducting crabon networks in the rubber system, while at high concentrations polyethylene acted as barriers and broke the conductivity network of CNP, which results in a decrease in conductivity. Nevertheless, conductivity value compared with conductive CNP/NBR composite is lower than that of CNP/poly ethylene/NBR epoxy nanocomposites, the nanocomposites conductivity maintained in static dissipative range.

### Stress–strain behavior and strain energy density

To investigate the influence of polyethylene on the mechanical properties of the nanocomposites, two samples were selected for such comparison. The first sample represents NBR loaded 0.2 vol % of CNP (percolation concentration) and the second sample contains NBR loaded 0.2 vol % of CNP and 3 vol% of polyethylene (optimum concentration).

Figure 3 shows the stress–strain curves obtained for NBR/CNP and NBR/PE/CNP. It is clear that the addition of polyethylene to the nanocomposite improves both of modulus of elasticity and strain at break by while decrease the stress at break. The modulus of elasticity is increased from 4.2 to 6.5 MPa, the strain at break is increased from 1.6 to 1.9 and the stress at break is decreased from 19.7 to 18.8 MPa.

The energy absorbed per unit volume ($W$) in deforming the rubber composites to a strain ε is simply the area under the stress–strain curve and can be written as[24]:

$$W = \oint \sigma(\varepsilon)d\varepsilon, \tag{2}$$

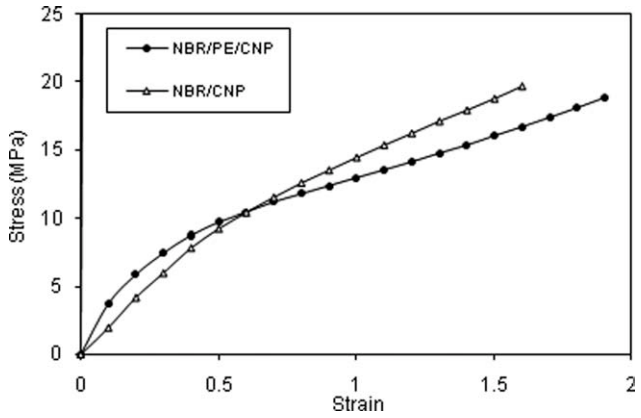


**Figure 3** The stress–strain curves for nanocomposites with and without polyethylene.

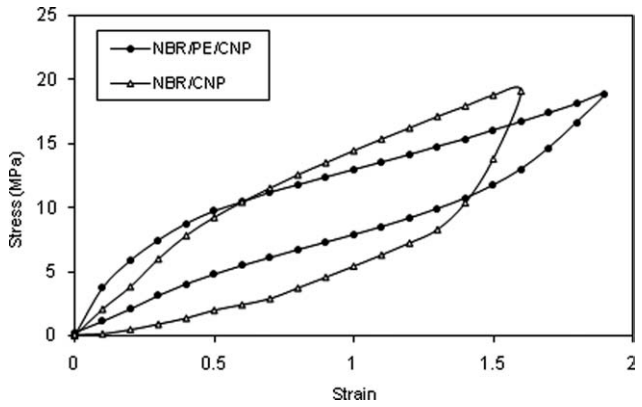


**Figure 4** The experimental stress–strain curves for loading and unloading at first cycle.

where σ (ε) is the stress as a function of the strain. Obviously, the higher the area under stress–strain curve, the higher the energy absorption capacity. The energy absorbed per unit volume ($W$) for NBR/CNP and NBR/PE/CNP is equal 11.15 and 12.47 MJ/m$^3$, respectively. It is apparent that the stored energy for nanocomposite with polyethylene is larger than that without it. Thus the addition of polyethylene enhances the mechanical properties the nanocomposites.

### Cyclic loading–unloading and dissipation energy

Figure 4 shows the experimental stress–strain curves for loading and unloading at first cycle for the samples. The cyclic stress–strain behavior observed upon deformation typically includes a significant strain energy contribution and the area enclosed by the hysteresis loop corresponds to the dissipated energy for each cycle. For any given cycle ($N$), the dissipated energy is given by[25]:

$$\Delta E(N) = \oint \sigma d\varepsilon = \int_0^{\varepsilon_{max}} [\sigma_{id}(N,\varepsilon) - \sigma_{ul}(N,\varepsilon)] d\varepsilon, \quad (3)$$

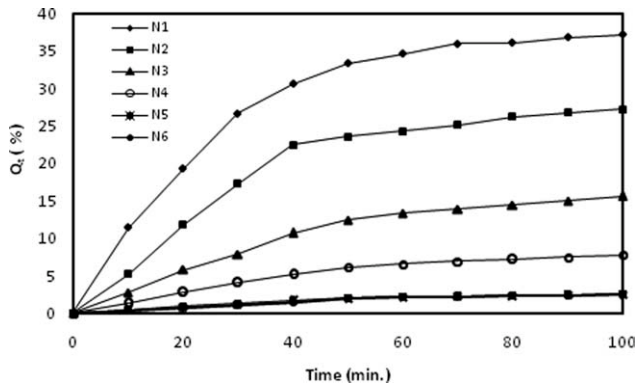


**Figure 5** Percent mass uptake for NBR loaded different concentrations of CNP in gasoline solvent.

where $\varepsilon_{max}$ is the maximum strain, $\sigma_{ld}$ is the loading stress, and $\sigma_{ul}$ is the unloading stress. The dissipated energy for nanocomposites with and without polyethylene is obtained and its value for first cycle is 0.61 and 0.97 MJ/m$^3$, respectively. It is clear that the addition of polyethylene to the nanocomposites reduces the rate of damage as well as the friction between CNP and rubber matrix.

### Diffusion profile

Data from sorption studies are presented as plots of the percentage uptake of the penetrant against time. Sorption plot for nanocomposites is presented in Figure 5. The percentage of solvent uptake gradually increases with time and then reaches an equilibrium value. This is the trend shown in all nanocomposites. However, there is variation in the equilibrium sorption value as well as the time taken to attain the equilibrium for each sample. The attainment of sorption equilibrium was found to be much quicker in the case rubber loaded small amounts of CNP. The solvent uptake is found to be high for green rubber but it is low for rubber loaded high concentration of CNP. Equilibrium extent of swelling and the rate of solvent uptake for all nanocomposites have been analyzed with various parameters related to the solvents such as molar volume, solubility parameter, density, and molecular weight. However, it was found that correlation exists only with the solubility parameter of the solvents for the present polymer-solvent systems. This is shown in Table III.

### Mechanism of sorption

The dynamic sorption data of the polymer-solvent systems for a circular geometry of the sample before 50% equilibrium sorption have been fitted to the following empirical formula.[26]

$$\frac{Q_t}{Q_\infty} = kt^n, \quad (4)$$

where $Q_t$ and $Q_\infty$ are the mole percent increase in sorption at time $t$ and at equilibrium, respectively. To investigate the type of diffusion mechanism, the sorption data of the penetrant-polymer systems have been analyzed in terms of the empirical relation.

**TABLE III**
**Equilibrium Uptake of Gasoline Solvent by Nanocomposites**

| Sample | N1 | N2 | N3 | N4 | N5 | N6 |
|---|---|---|---|---|---|---|
| $Q_\infty$ (%) | 37.2 | 27.4 | 15.6 | 7.8 | 2.6 | 2.5 |

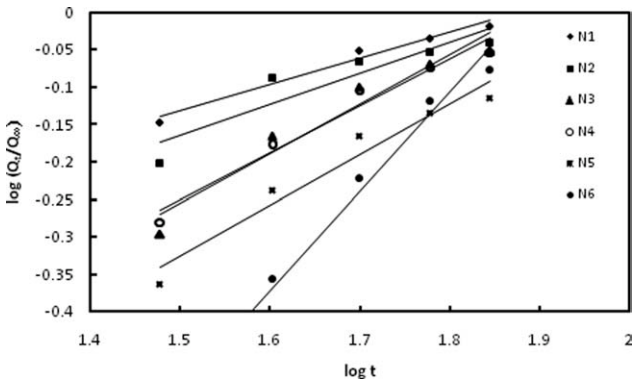


**Figure 6** Plot of log $Q_t/Q_\infty$ versus log $t$ for nanocomposites in gasoline solvent.

$$\log \frac{Q_t}{Q_\infty} = \log k + n \log t, \tag{5}$$

The parameter $k$ and $n$ have been determined from a least square fit of the experimental log $Q_t/Q_\infty$ versus log $t$ (Fig. 6). The values are tabulated in Table IV.

Constant $k$ depends on the structural features of the polymer system and its interaction with the solvent used. The value of $n$ provides information about the mechanism of solvent transport. When the value of $n$ is 0.5, the sorption mechanism is Fickian and the rate of polymer chain relaxation is higher than the diffusion rate of the penetrant. When $n = 1$, the diffusion mechanism is said to be non-Fickian where the chain relaxation is slower than the solvent diffusion. If the values lie between 1 and 0.5, then the mechanism is said to follow anomalous trend where the polymer chain relaxation rates and the solvent diffusion rate are similar. The values of $n$ in the present study vary between 0.65 and 0.97 in the investigated temperature range. For nanocomposites like N1 and N2 the values of $n$ are found to be in between 0.65 and 0.77 which suggest that the transport mechanism is very close to Fickian mode where the rate of chain relaxation tends to be greater than the diffusion rate of the penetrant. For N3, N4, N5, and N6 the values of $n$ are higher but less than one suggesting anomalous sorption behavior where the rate of relaxation and diffusion are comparable. This anomalous behavior for the solvents may be due to the interaction of the polar and nonpolar segments of the polymer matrix almost equally with the solvent. Thus, time will be taken by the NBR hard segment to respond to the swelling stress and rearrange them to accommodate the solvent molecules. Combining effect of the polarity of the solvent and size of the penetrant as well as the presence of both polar and nonpolar segments in nanocomposites determine the value of $k$. These values of $k$ were found increase as the amount of CNP increase in the rubber composite.

**Diffusion coefficient**

Diffusion through a polymer occurs when small molecules pass through voids and other gaps between the polymer molecules. Diffusion rate will, therefore, depend on the size of the small molecules and the size of the gap in the polymer. The latter depends on a large extent on the physical state of the polymer, that is, whether glassy, rubbery or crystalline. For Fickian transport the rate of approach to equilibrium swelling can be characterized by a diffusion coefficient. Fick's law is the most suitable equation for defining the diffusion coefficient. The effective diffusivity or diffusion coefficient ($D$) of the polymer-solvent system is a kinetic parameter which can be calculated from the initial linear portion of the sorption curves using the following equation.[27]

$$\frac{Q_t}{Q_\infty} = 1 - \left(\frac{8}{\pi^2}\right) \sum_{n=0}^{\infty} \left( \frac{e^{-\left(\frac{D(2n+1)^2\pi^2 t}{h^2}\right)}}{(2n+1)^2} \right), \tag{6}$$

where $Q_t$ and $Q_\infty$ are the mass of solvent uptake at time $t$ and at equilibrium, respectively, $h$ is the initial sample thickness. Although this equation can be solved readily, it is instructive to examine the short time limiting expression as well.[28]

$$\frac{Q_t}{Q_\infty} = \left(\frac{4}{\pi^{1/2}}\right)\left(\frac{Dt}{h^2}\right)^{1/2}. \tag{7}$$

From a plot of $Q_t$ versus $t^{1/2}/h$, a single master curve is obtained which is initially linear. Thus, $D$ can be calculated from a rearrangement of eq. (7) as

$$D = \pi \left( \frac{h\theta}{4Q_\infty} \right)^2, \tag{8}$$

where $\theta$ is the slope of the nearly linear portion of the sorption curve, that is, before the attainment of 50% of equilibrium uptake (Fig. 1) and $Q_\infty$ is the mole percent increase in sorption at equilibrium. From this equation, it is understood that $D$ is directly proportional to the slope and inversely proportional to the maximum solvent uptake. Because of considerable swelling in a short period, a swelling correction is necessary to get correct diffusion coefficient, known as the intrinsic diffusion coefficient

**TABLE IV**
**Swelling Characteristics in Terms of $k$ and $n$ Values of Nanocomposites at 30°C**

| Sample parameter | N1 | N2 | N3 | N4 | N5 | N6 |
|---|---|---|---|---|---|---|
| $n$ | 0.65 | 0.77 | 0.84 | 0.89 | 0.94 | 0.97 |
| $k$ | 0.35 | 0.43 | 0.56 | 0.74 | 0.81 | 1.02 |

**TABLE V**
**Diffusion, Sorption, and Permeation Coefficients of Gasoline Solvent in the Nanocomposites**

| Sample parameter | N1 | N2 | N3 | N4 | N5 | N6 |
|---|---|---|---|---|---|---|
| $D^*$ ($10^2$ cm$^2$ s$^{-1}$) | 11.2 | 7.1 | 3.4 | 1.5 | 0.6 | 0.5 |
| $S$ | 3.1 | 2.6 | 1.4 | 0.8 | 0.7 | 0.6 |
| $P$ ($10^2$ cm$^2$ s$^{-1}$) | 34.7 | 18.5 | 4.8 | 1.2 | 0.4 | 0.3 |

($D^*$). This can be calculated using the following equation[29]:

$$D^* = \frac{D}{\varphi^{T/E}}, \tag{9}$$

where $\phi$ is the volume fraction of the CNP. The estimated values of the intrinsic diffusion coefficient of samples are given in Table V. The variation in $D^*$ value depends on the nature of the crosslink. Normally, the diffusion coefficient values decrease with increasing the concentration of CNP. All the nanocomposites show wide variations in the $D^*$ values as a result of the increase of CNP concentration into rubber matrix as shown in Table V. The highest value is shown by N1 and the lowest value is observed in N6.

To get a better understanding on the strength of interaction between polymer and solvent, the sorption coefficient, ($S$), which is a thermodynamic parameter, has been calculated using the relation,

$$S = \frac{M_S}{M_P}, \tag{10}$$

where $M_S$ is the mass of the penetrant molecules at equilibrium swelling and $M_P$ is the initial mass of the polymer sample.[30] It is found that $S$ is maximum for N1 system and minimum for N6 system (Table V). The higher value for N1 is an indication of the better accommodation of the solvent molecules due to favorable interaction with the hard domains as well as the soft NBR matrix and also due to the small size of the penetrant. The minimum value for N6 is explained by the fact that the solvent is unable to interact with the NBR segments, due to the high concentration of CNP which are involved in the formation of domains resulting in physical crosslinking.

**TABLE VI**
**Thermodynamic Parameters for the Solvent Uptake by the Nanocomposites**

| Sample parameter | N1 | N2 | N3 | N4 | N5 | N6 |
|---|---|---|---|---|---|---|
| $\Delta H^o$ (KJ mol$^{-1}$) | 0.29 | 0.25 | 0.24 | 0.23 | 0.05 | 0.04 |
| $\Delta S^o$ (J mol$^{-1}$ K$^{-1}$) | 0.62 | 0.79 | 0.86 | 0.97 | 1.61 | 1.64 |
| $\Delta G^o$ (KJ mol$^{-1}$) | 0.34 | 0.29 | 0.19 | 0.11 | 0.08 | 0.07 |
| $K_S$ | 0.21 | 0.19 | 0.15 | 0.11 | 0.09 | 0.05 |

Since the physical crosslinks are intact the NBR segments held by them could absorb solvent only to limited levels.

The process of permeation is a combined effect of diffusion and sorption and thus the permeability coefficient, ($P$) depends on both $D$ and $S$. Therefore, $P$ can be calculated using eq. (11).

$$P = \mathrm{DS} \tag{11}$$

This relationship holds for the permeation process when the material obeys Fick's law and Henry's law. $P$ values in gasoline solvent are given in Table V. It is found that the value is highest for N1 and N2 and minimum for N6. The $D^*$ is the average capacity of the solvent molecules to move among the polymer chain segments and $S$ is a thermodynamic function which depends on the equilibrium sorption value. $P$ reflects the net effect of sorption and diffusion. Compared to $D^*$ and $P$, the value of $S$ is higher and this indicates a large tendency of solvent to dissolve or sorb into the polymer. From this, it is possible to conclude that sorption predominates over diffusion in the permeation process of the system under study.

### Thermodynamic parameters

Thermodynamic sorption constant, ($K_S = Q_s/C_s$) gives a further understanding of the uptake of solvent by polymer.[31] The effect of nanocomposites characteristics on the $K_S$ value can be seen in Table VI. N1 showed a high $K_S$ value. The trend is exactly same as that for $Q_\infty$ values. $K_S$ values decrease from N1 to N6. Enthalpy ($\Delta H^o$) and entropy ($\Delta S^o$) values were calculated by plotting ln $K_S$ versus $1/T$ as per eq. (17) for the different nanocomposites (Fig. 7). The corresponding free energy ($\Delta G^o$) values could be obtained from these data.

$$\ln K_S = \frac{\Delta S^0}{R} - \frac{\Delta H^0}{RT}. \tag{12}$$

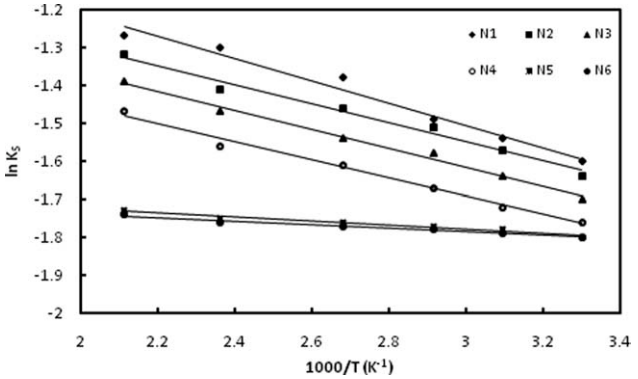


**Figure 7** Plot of ln $K_S$ versus $1/T$ for the nanocomposites.

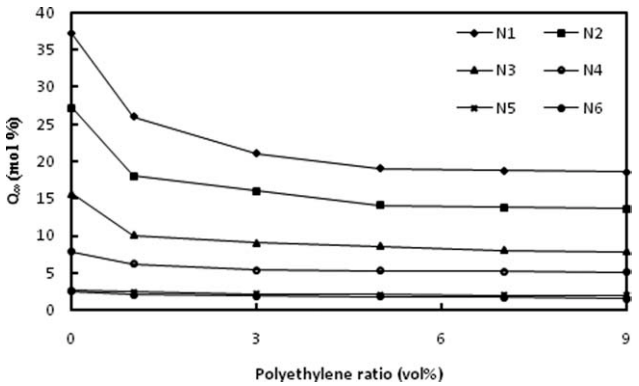


**Figure 8** Effect of polyethylene ratio on the equilibrium swelling.

From the slope and intercept of the plot, $\Delta S^o$ and $\Delta H^o$ values were obtained. The $\Delta G^o$ of the process was calculated from these values. It may be noted that for all nanocomposites, the values of $\Delta H^o$ are positive and they vary from 0.29 to 0.04 kJ $mol^{-1}$. This means the sorption of solvent is also giving an endothermic contribution to the process. Hence, it was dominated by Henry's law mode, that is, the sorption proceeded through the creation of new sites or pores in the polymer. As shown in Table VI, $\Delta S^o$ values are negative for all the block copolymers, which suggest that the structure of the solvent molecules was retained even in the sorbed state. $\Delta S^o$ values are in the range 0.62–1.64 J $mol^{-1}$ $K^{-1}$. However, the $\Delta G^o$ values are positive and small. It can be concluded that the sorption process is controlled predominantly by thermodynamic factors.

### The effect of polyethylene ratio on transport behavior

Figure 8 shows the variation in equilibrium sorption with polyethylene ratio loaded the nanocomposites. The sorption values decreased to half in N1, N2, and N3 as the polyethylene ratio increases from 10 to 50 phr. About 35% decrease is observed in N4. Other nanocomposites N5 and N6 show only small decrease in the equilibrium sorption. In all cases, equilibrium sorption decreases with increase in the polyethylene ratio. As the polyethylene ratio is high the excess of polyethylene favors more crosslinking in the polymer systems. Higher level of crosslinking causes lower solvent uptake. The Fickian and anomalous behavior for nanocomposites described previously are valid at all polyethylene ratios, which indicate that the diffusion and relaxation phenomena are dependent on polyethylene ratio. An increase in the $n$ value with low polyethylene ratio is observed. However, the increase is observed within the limit of the anomalous region only.

Figure 9 shows the variation of $P$ with the polyethylene ratio. It is found that the value decreases almost three times with the increase in polyethylene ratio in all nanocomposites. As this ratio increases the level of crosslinking in the sample is also increase which minimize free volume and leads to a decrease in the diffusion process. Thus, solvent penetration through the nanocomposites is reduced at high polyethylene ratio. Although the general trend is a decrease in the above properties with the increase in polyethylene ratio, significant increase is observed at the lowest value of polyethylene, viz. 3 vol %. This is very pronounced in N1, N2, and N3 as evidenced from the respective plot. Hence this value of polyethylene ratio seems to be the optimum and it signifies the minimum required crosslinking in the samples to show lower level of solvent permeation.

The crosslinks between polymer chains usually resist the solvent molecules to penetrate in the polymer matrix. To observe the effect of polyethylene content on the penetration of liquid molecules, crosslink density (defined as the number of moles of crosslinks per unit volume) of nanocomposites are calculated by the Flory-Rehner equation.[32]

$$-[\ln(1-V_r)+V_r+\chi V_r^2]=V_o n(V_r^{1/3}-V_r/2), \quad (13)$$

where, $n$ is the crosslink density; $V_r$ and $V_0$ are the volume fraction of nanocomposite in the swollen mass and molar volume of solvent respectively; $\chi$ is the polymer-solvent interaction parameter. The volume fractions ($V_r$) of the nanocomposite in the swollen mass are reverse of the swell ratio,[33] i.e., $V_r = 1/q$. The value of $\chi$ could be obtained from the Flory Huggins's equation.

$$\chi = 0.34 + V_o(\delta_s - \delta_p)^2/RT, \quad (14)$$

where, $\delta_s$ and $\delta_p$ are solubility parameter of solvent and polymer respectively.[34] Figure 10 represents the

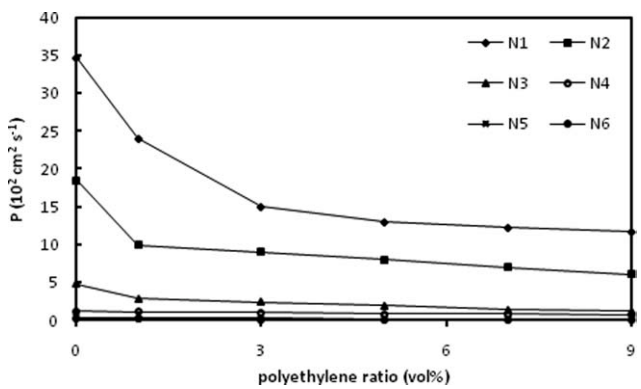


**Figure 9** Effect of polyethylene ratio on the permeation coefficient.

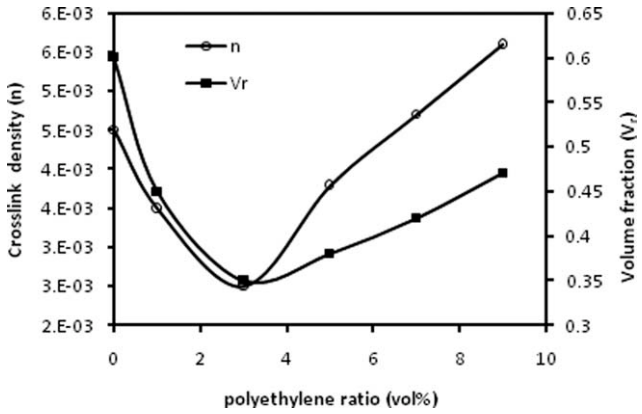


**Figure 10** Effect of polyethylene ratio on the volume fraction and crosslink density of NBR nanocomposites.

influence of polyethylene content on volume fraction ($V_r$) and crosslink density ($n$) of NBR during swelling and its nanocomposites with CNP. It shows that the volume fraction, $V_r$, and crosslink density, $n$, of the nanocomposite in the swollen mass decrease up to 3 vol %. Subsequently, it is followed by continuous increase in the volume fraction and crosslink density up to 9 vol % filler contents. But in both the cases, $V_r$ and $n$ is lesser in NBR/CNP nanocomposites compared to the neat NBR. It is expected that at the initial stage, presence of higher exfoliated clay level up to 3 vol % reduce the "bound polymer" and increase the free volume in the NBR matrix. When solvent molecules penetrate in to the matrix, they can spread apart the flexible polymer chains and imparts high chain mobility. As a result, the solvent can easily penetrate the larger absorption site of the elongated polymer chain and the solvent uptake is more. However, increase in intercalation level above 3 vol % filler inhibits the penetration of solvent molecules through bridging flocculation.

## CONCLUSION

CNP loaded NBR nanocomposites were developed. The percolation threshold concentration (0.2 vol %) was determined. Electrical conductivity results revealed that direct current conductivity decreases with polyethylene addition into CNP/NBR composites. Nanocomposite with only 3 vol % of polyethylene content was electrically conductive, whereas the other concentrations above it were not conductive. The mechanical measurements depicted that the addition of polyethylene by 3 vol % to the nanocomposite improve the modulus of elasticity as well as strain energy density. The cyclic fatigue showed that the polyethylene reduce the rate of damage of nanocomposites. Nanocomposites with low loading of CNP were found to show the maximum amount of uptake by gasoline solvent. Transport of these nanocomposites is found to follow anomalous behavior where the rate of relaxation and diffusion are comparable. This may be due to the interaction of the polar and nonpolar segments of the polymer matrix almost equally with the solvent. The transport follows first order kinetics with highest rate constant. All the nanocomposites show wide variations in the $D^*$, $S$, and $P$ values at low concentrations of CNP. The highest value is shown by N1 and the lowest value is observed for N6. The high value for N1 is an indication of the better accommodation of the solvent molecules due to favorable interaction with the hard domains as well as the soft NBR matrix and also due to the small size of the penetrant. The $\Delta H^o$ and entropy ($\Delta S^o$) of the sorption process show highest values in N1, N2, and N3 and lowest value in N6. Free energy of the process is positive suggesting that the sorption of solvent is giving an endothermic contribution to the process. It can be concluded that the process is controlled predominantly by thermodynamic factors rather than the penetrant size. The polyethylene ratio is found to play an important role in the solvent transport. The sorption is found to decrease with increase in the polyethylene ratio irrespective of the nature of the solvent.

## References

1. Ciobanu, C.; Han, X.; Cascaval, C.; Guo, F.; Rosu, D.; Ignat, L.; Moroi, G. J Appl Polym Sci 2003, 87, 1858.
2. Elliott, J. E.; Macdonald, M.; Nie, J.; Bowman, C. N. Polymer 2004, 45, 1510.
3. McBride, J. S.; Massaro, T. A.; Cooper, S. L. J Polym Sci 1979, 23, 20.
4. Yang, Y.; Huang, Y.; Chen, Y.; Wang, D.; Liu, H.; Hu, C. J Appl Polym Sci 2004, 91, 2984.
5. Kendaganna Swamy, B. K.; Siddaramaiah, R. J Hazard Mater 2003, 99, 177.
6. Ravindran, T.; Nayar, M. R. G.; Francis, D. J. J Appl Polym Sci 1988, 35, 1227.
7. Paul, C. J.; Nair, M. R. G.; Neelakantan, N. R.; Koshy, P.; Idage, B. B.; Bhelhekar, A. A. Polymer 1998, 6861, 26.
8. Paul, C. J.; Nair, M. R. G.; Koshy, P.; Idage, B. B. J Appl Polym Sci 1999, 74, 706.
9. Paul, C. J.; Nair, M. R. G.; Neelakantan, N. R.; Koshy, P. Polym Eng Sci 1998, 31, 440.
10. Gopakumar, S.; Paul, C. J.; Nair, M. R. G. J Mater Sci (Poland) 2005, 23, 227.
11. Ravindran, T.; Nayar, M. R. G.; Francis, D. J. J Appl Polym Sci 1991, 42, 325.
12. MacDiarmid, A.G. Short Course on Conductive Polymers; SUNY: New Platz, New York, 1985.
13. Heinze, J. Top Curr Chem 1990, 152, 1.
14. Heeger, A. J. J Phys Chem B 2001, 105, 8475.
15. Abdel-Bary, E. M.; Amin, M.; Hassan, H. H. J Polym Sci Polym Chem 1974, 12, 2651.
16. Al-Lawindy, A. M. Y.; Abdel Kader, K. M.; Mahmoud, W. E.; Hassan, H. H. Polym Int 2002, 51, 601.
17. Mahmoud, W. E.; El Eraki, M. H.; El-Lawindy, A. M. Y.; Hassan, H. H. J Phys D Appl Phys 2006, 39, 541.
18. Mahmoud, W. E.; El Eraki, M. H.; El-Lawindy, A. M. Y.; Hassan, H. H. J Phys D Appl Phys 2006, 39, 2427.

19. Mahmoud, W. E.; Mansour, S. A.; Hafez, M.; Salam, M. A. Polym Degrad Stabil 2007, 92, 2011.
20. Zhang, J.; Han, H.; Wu, S.; Xu, S.; Yang, Y.; Zhou, C.; Zhao, X. Solid State Ionics 2007, 178, 1595.
21. Al-Ghamdi, A. A.; El-Tantawy, F.; Abdel Aal, N.; El-Mossalamy, E. H.; Mahmoud, W. E. Polym Degrad Stabil 2009, 94, 980.
22. Zois, H.; Apekis, L.; Omasova, M.1999. Electrical Properties and Percolation Phenomena in Carbon Black Filled Polymer Composites, 10th International Symposium on Electrets, pp 529–532.
23. Flandin, L.; Bréchet, Y.; Canova, G. R.; Cavaillé, J. Y. Mater Sci Eng 1999, 7, 865.
24. Mahmoud, W. E.; El-Lawindy, A. M. Y.; El Eraki, M. H.; Hassan, H. H. Sensors Actuators A 2007, 136, 229.
25. El Eraki, M. H. I.; El Lawindy, A. M. Y.; Hassan, H. H.; Mahmoud, W. E. J Appl Polym Sci 2007, 103, 2837.
26. Bajsic, G.; Rek, V. J Appl Polym Sci 2001, 79, 864.
27. Aminabhavi, T. M.; Munnoli, R. S. J Hazard Mater 1994, 38, 223.
28. George, S. C.; Ninan, K. N.; Thomas, S. Polym Compos 1999, 7, 343.
29. Mathai, A. E.; Singh, R. P.; Thomas, S. J Mater Sci 2002, 202, 35.
30. Harogoppad, S. B.; Aminabhavi, T. M. Macromolecules 1991, 25, 2595.
31. Siddaramaiah, R.; Roopa, S.; Guprasad, K. H. J Appl Polym Sci 2003, 88, 1366.
32. Flory, P. J. Principles of Polymer Chemistry; Cornell University: Ithaca, New York, 1953, p 576.
33. Pramanik, M.; Acharya, H.; Srivastava, S. K. Macromol Mater Eng 2004, 289, 562.
34. Ratanarat, K.; Nithitanakul, M.; Martin, D. C.; Magaraphan, R. Rev Adv Mater Sci 2003, 5, 187.